Energy & Environmental Science

RSC Publishing

COMMUNICATION

View Article Online
View Journal | View Issue

A paper-based nanogenerator as a power source and active sensor†

Cite this: *Energy Environ. Sci.*, 2013, **6**, 1779

Received 21st February 2013
Accepted 27th March 2013

DOI: 10.1039/c3ee40592c

www.rsc.org/ees

Qize Zhong,‡[a] Junwen Zhong,‡[a] Bin Hu,[a] Qiyi Hu,[a] Jun Zhou*[a] and Zhong Lin Wang[bc]

Paper-based functional electronic devices endow a new era of applications in radio-frequency identification (RFID), sensors, transistors and microelectromechanical systems (MEMS). As an important component for building an all paper-based system that can work independently and sustainably, a paper-based power source is indispensable. In this study, we demonstrated a paper-based nanogenerator (pNG) that can convert tiny-scale mechanical energy into electricity. The pNG relies on an electrostatic effect, and the electrostatic charges on the paper were generated by the corona method. The instantaneous output power density of a single-layered pNG reached ~90.6 μW cm^{-2} at a voltage of 110 V, and this instantaneously illuminated 70 LEDs. In addition, by sticking the pNG to a movable object, such as the page of a book, the power harvested from the mechanical action of turning the page can drive an LED, which presents its outstanding potential in building paper-based, self-powered systems and as active sensors.

Broader context

Technology advances in flexible electronics have promoted the demand for cheap, lightweight, recyclable and environmentally benign energy generators that can supply power independently and sustainably. In this work, we design and fabricate a paper-based nanogenerator (pNG) using an electrostatic effect. A maximum peak power density of ~90.6 μW cm^{-2} was generated, and the pNG directly powered 70 LEDs connected in series with a turn-on voltage of up to 110 V. Moreover, the pNG could be attached onto various movable objects to harvest energy; the pNG stuck to the page of a book, for instance, could harvest energy from the mechanical action of turning the pages to light up two blue LEDs that were connected in antiparallel. The successful synthesis of this pNG paves the way in harvesting energy based on electrostatic actuation and this study presents the significant potential applications of a paper-based self-powered system as an energy source or as an active sensor.

Introduction

Paper is one of the most important inventions in human civilization and it has been used for centuries.[1] In the past decade, by virtue of it being cheap, lightweight, recyclable, disposable and environmentally benign, paper has been endowed with new applications in disposable and flexible electronics, which extends its range of applications from conventional purposes to use in novel electronic devices such as RFIDs, sensors, transistors and MEMS.[2–10] It is an important component for building all paper-based systems that can work independently and sustainably, and energy generators based on paper can have a diverse range of applications.[11,12] In this regard, designing an integratable paper-based energy generator, that can harvest energy from an ambient energy source and convert it into electricity, is an effective approach for building low-cost, green and disposable self-powered devices and systems.

Irregular mechanical energies, such as human body activity, breath, ambient noise and airflows, are probably the most common energy sources in our living environment, but they are often ignored. Piezoelectric nanogenerators,[13–21] triboelectric nanogenerators (TENGs)[22–26] and electrostatic generators[27–29] have been demonstrated to be effective technologies to convert irregular mechanical energy to electricity. In this work, we design and fabricate a paper-based nanogenerator (pNG) using an electrostatic effect. A maximum peak power density of ~90.6 μW cm^{-2} was generated, and this directly powered 70 LEDs connected in series with a turn-on voltage of up to 110 V. Moreover, the pNG could be attached onto various movable objects to harvest energy; the pNG stuck to the page of a book, for instance, could harvest energy from the mechanical action of turning the pages to light up two blue LEDs that were connected in antiparallel. This study opens a new field of research

[a]*Wuhan National Laboratory for Optoelectronics, School of Optical and Electronic Information, Huazhong University of Science and Technology, Wuhan, 430074, China. E-mail: jun.zhou@mail.hust.edu.cn*

[b]*School of Materials Science and Engineering, Georgia Institute of Technology, Atlanta, Georgia 30332-0245, USA*

[c]*Beijing Institute of Nanoenergy and Nanosystems, Chinese Academy of Sciences, Beijing, China*

† Electronic supplementary information (ESI) available: additional Fig. S1–S3 and videos 1–3. See DOI: 10.1039/c3ee40592c

‡ Authors with equal contribution.

not only in paper applications, but also in the development of new sources of energy for a range of applications in sensing and actuating.

Experimental

Fabrication of Ag–paper and PTFE–Ag–paper

The fabrication started by depositing a ~100 nm Ag layer by thermal evaporation (ZHD-300 M2, Technol, China) onto a piece of commercial printing paper (GOLDEN COLOR, China) to form Ag–paper. Then, the Ag–paper was spin-coated with a non-purified polytetrafluoroethylene (PTFE) suspension (Aladdin) three times at 3000 rpm for 30 s to form PTFE–Ag–paper. The PTFE–Ag–paper was thermally cured in an oven at 150 °C for 10 h, and then polarized in the direction perpendicular to the paper *via* the corona method[30–33] at a 25 kV high voltage for 20 min.

Assembly of the pNG

The pre-prepared PTFE–Ag–paper and Ag–paper pieces were assembled to make the pNG. To assemble the two components, the PTFE side of the PTFE–Ag–paper was orientated so that it was facing the Ag layer of the Ag–paper, and the edges of the two pieces were fixed along the length axis using Kapton tape, forming an arch-shaped device with an effective area of 2.5 cm × 2 cm.

Characterization

The morphology of the samples was imaged using a high-resolution field emission scanning electron microscope (FEI Nova NanoSEM 450). The output characteristics of the pNG were measured using a Stanford low-noise current preamplifier (Model SR570) and a NI PCI-6259. In the test, the pNG was attached to an elastic plastic sheet, one end of which was tightly fixed to an *x*–*y*–*z* mechanical stage (3D Stage). A resonator (JZK, Sinocera, China) was utilized to periodically trigger the device with a swept controllable frequency and amplitude that was controlled by a signal generator (YE 1311-D, Sinocera, China).

Results and discussion

The detailed fabrication process of the pNG is schematically provided in Fig. 1a. Ag was evaporated onto a commercial printing paper that served as a substrate to form an Ag–paper structure (Fig. 1b). A comparison of the energy dispersive X-ray (EDX) spectra before and after evaporation proved the existence of Ag on the paper (Fig. S1†). Then, a 3 cm × 2 cm sample of Ag–paper was spin-coated with PTFE, which coated the Ag layer and left a space for the electrode. Fig. 1c and d present cross-sectional and top view SEM images after the PTFE coating, respectively. The thickness of the PTFE film is ~80 μm and the surface is rather rough. After thermally curing in an oven, the as-fabricated PTFE–Ag–paper was polarized *via* the corona method, which resulted in a net negative electrostatic charge (Q) remaining on the PTFE surface. It is reported that theoretically, the charges on the PTFE surface can be retained for hundreds of years,[29,34] which guarantees the sustainable active status of the device within the period of our measurements and applications. The two components of the pNG were assembled by facing the PTFE of the PTFE–Ag–paper to the Ag layer of the Ag–paper, and fixed the edges of the two sheets along the length axis using Kapton tape, forming an arch-shaped device with an effective area of 2.5 cm × 2 cm (step IV of Fig. 1a).

Fig. 2a–c schematically illustrate a simplified equivalent generation mechanism model of the pNG with an external load of R. In general, the pNG could be considered as an ideal flat-panel capacitor by ignoring the edge effect. In the original state, the inner surface of the PTFE was negatively charged with a charge density of σ, and simultaneously the Ag electrodes of the PTFE–Ag–paper and the Ag–paper were positively charged owing to the electrostatic induction shown in Fig. 2a. Assuming the electrostatic charges on the surface of the PTFE and Ag electrodes are uniformly distributed, at any equilibrium state, the surface charge density σ_2 on the Ag–paper electrode is given as follows;[27]

$$\sigma_2 = -\frac{\sigma d_1}{d_2\varepsilon_{rp} + d_1} \quad (1)$$

where d_1 is the thickness of the PTFE, ε_{rp} is the relative permittivity of the PTFE with a value of ~1.93,[34] and d_2 denotes the distance between the PTFE surface and the Ag layer of the Ag–paper. As mentioned above, the surface charge density σ of the PTFE could be retained for a long time without any leakage, and hence σ_2 can be considered as a function of d_2 (see Fig. 2d). When the pNG was pressed (Fig. 2b), a reduction in the interlayer distance d_2 induces an increase in σ_2 according to eqn (1). This behavior resulted in an instantaneous positive current (we defined a forward connection for the measurement as a configuration with the positive end of the electrometer connected to the Ag electrode of the PTFE–Ag–paper).

In the reverse case, when the pNG was released (Fig. 2c), the device reverted back to its original arched shape and the interlayer distance d_2 increased, resulting in a decrease in surface charge σ_2 according to Fig. 2d, and an instantaneous negative current was produced. This process shows that the deformation-induced variation of d_2 results in the redistribution of the charges between the electrodes across the load R, which generates an AC current through the load; in other words, the mechanical energy was converted into electricity. It is obvious that the peak current I is related to the measurement conditions, which is proportional to the varying frequency of the deformation under the same interlayer gap d_2. In addition, as illustrated in Fig. 2d, charge density σ_2 would also be influenced by the thickness of the spin-coated PTFE. Therefore, selecting the proper parameters for device fabrication is important to optimize the performance of the pNG.

The typical output characteristics of the pNG were systematically studied by periodically pressing and releasing at a controlled frequency and amplitude. Fig. 3a illustrates the output performance of the pNG under different external loads at a frequency of 40 Hz and degree of deformation (~1.5 mm). As we can see, the load peak voltage increased with external load resistance, from ~7 V at 1 MΩ to ~230 V at 200 MΩ. However,

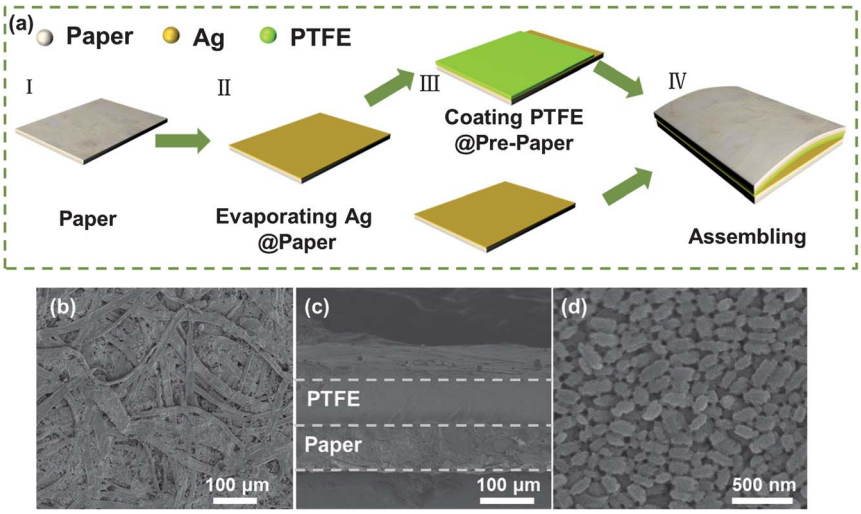

Fig. 1 (a) A schematic diagram illustrating the process of fabricating an arch-structured pNG. SEM images of (b) the paper coated with a Ag layer, (c) the cross-sectional and (d) the top view of the Ag–paper after spin-coating with PTFE.

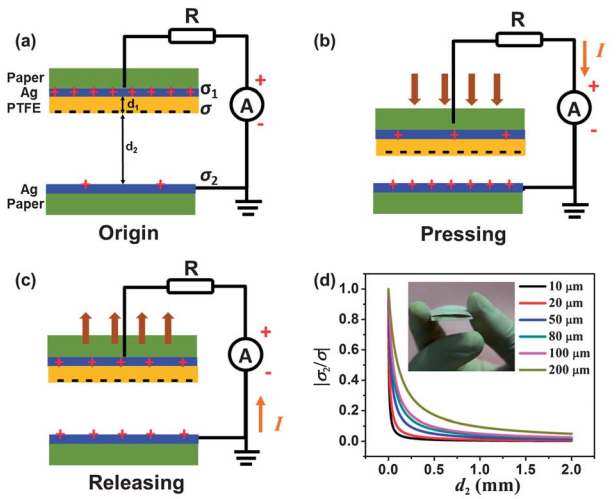

Fig. 2 The mechanism of the pNG with an external load of R when the device is in the (a) original, (b) pressing and (c) releasing state, respectively. (d) The relationship of the ratio between the induced charge density (σ_2) on the Ag layer of the Ag–paper and the charge density (σ) on the PTFE with different thickness. The inset depicts the digital photography of an arch-structured flexible pNG.

the slope of the output voltage curve reduced gradually and the output voltage became saturated at the open-circuit voltage when the resistance became infinitely large. The peak current followed an opposite trend decreasing from ~10 μA to ~1.2 μA under the same external loads. Accordingly, the maximum output power density of ~90.6 μW cm^{-2} was obtained at a corresponding load of ~40 MΩ. This result indicates that an increase in the load resistance to a value of hundreds of MΩ would lower the output current approaching 1 μA, which is not large enough to directly drive many commercial personal electronic devices.

The stability of the pNG was also studied and the result is shown in Fig. S2.† No attenuation of the output current was observed. Unexpectedly, the device showed a slow increasing output value in comparison to its initial performance. This phenomena can be attributed to the triboelectricity effect[22–26] which has been intensively studied. According to the triboelectric series,[35] when PTFE makes a direct contact with Ag, electrons will injected from Ag into PTFE until the saturation of the net negative charge is achieved at the PTFE surface.

To evaluate the performance of the optimized system, a pNG was attached to an elastic plastic sheet; one end of which was tightly fixed to an x–y–z mechanical stage, and the free-standing end of the plastic sheet was pressed and released periodically by a resonator as illustrated in the inset of Fig. S3.† At a controlled bending frequency of 40 Hz and an amplitude of ~1.5 mm, the pNG with a parallel resistance of 40 MΩ could instantaneously and continuously light up an LED pattern consisting of 70 commercial LEDs in series without using an energy storage unit (shown in the digital photograph in the inset of Fig. 3b and video 1†), and the I–V curve for the 70 LEDs depicted in Fig. S3† implied that the output voltage of the pNG was up to 110 V.

Another problem we may face is that, in spite of the ability to obtain a high output voltage and current for the pNG, the alternating current pulses cannot be used to directly power electric devices in most cases, as the devices often need a constant bias current or voltage. The storage unit, such as a supercapacitor,[36–43] capacitor or battery,[44–46] can store the pulse energy and later supply a regulated power. As illustrated in Fig. 3c and d, the electrical energy produced by the pNG was rectified and stored in a commercial capacitor (4.7 μF), and the upper inset depicts the equivalent circuit loop. The voltage across the capacitor was monitored during the charging process, and we found that the charging time from 0 V to 5 V could be less than 20 s when running the pNG under a triggering frequency of 40 Hz with an impelling amplitude of ~1.5 mm. The lower inset in Fig. 3d is the enlarged plot of the voltage curve, and the stepped increase of the capacitor voltage corresponds to the periodical press and release of the pNG, which are

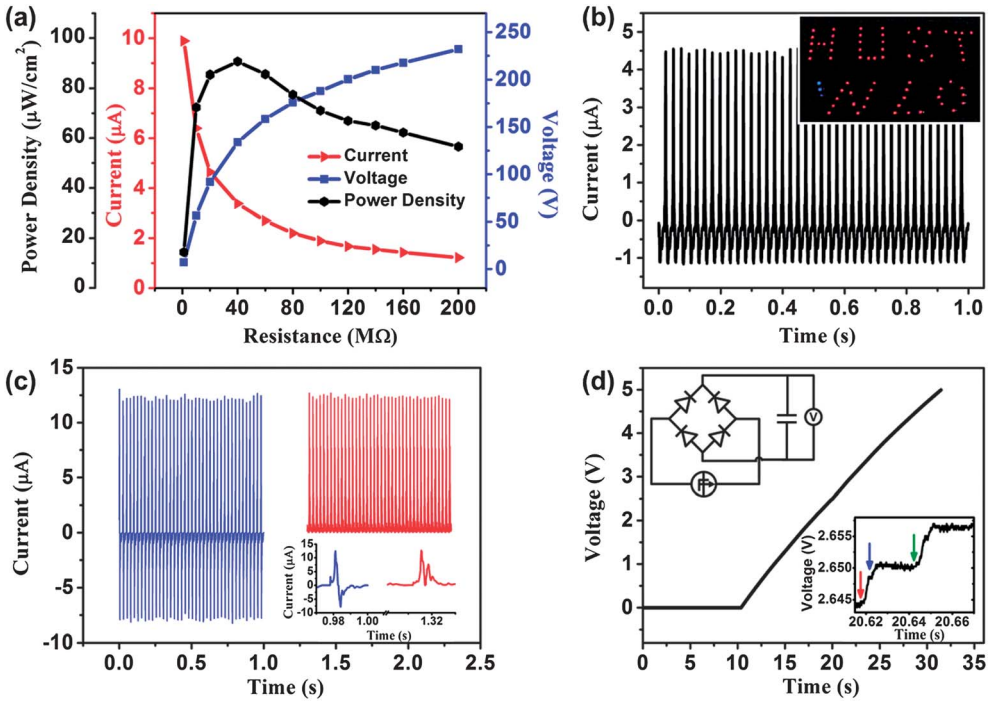

Fig. 3 The electrical performance of a pNG under different experiment conditions. (a) The output peak power density, current and voltage as a function of the load resistance for a given frequency of 40 Hz and an impelling amplitude of ~1.5 mm. (b) The current–time curve for the pNG as a power to directly drive 70 commercial LEDs. Inset depicts the digital photograph of the LED patterns of "HUST" and "WNLO" that are lit up by the pNG. (c) The output current of the pNG with and without rectification. The inset depicts the enlarged plot of the current. (d) The voltage charging curve of the capacitor for a given frequency of 40 Hz and an impelling amplitude of ~1.5 mm. The upper inset depicts the equivalent loop circuit for storing the electrical energy produced by the pNG. The lower inset shows an enlarged plot during charging.

marked by red and blue arrowheads, respectively, while the green arrowhead depicts the start of the next cycle of deformation.

Most vibration modes in nature are irregular and at a low frequency, such as human action. To extend the potential applications of the pNG by harvesting irregular energy, we successfully demonstrated the harvest of mechanical energy in turning a page of a book using the pNG in a practice situation. As shown in Fig. 4c, a pNG was attached onto a page of a book. When the page was turned over, the pNG could harvest the

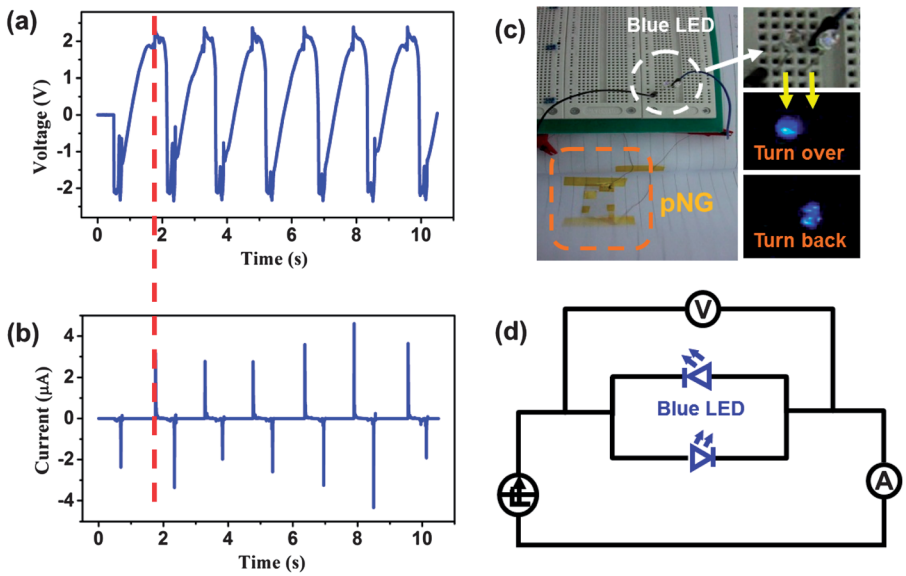

Fig. 4 The performance of a pNG attached to a page of a book. (a) The voltage across and (b) the current through the two blue LEDs connected in antiparallel driven by turning a book page. (c) The digital photograph of the prototype of the energy harvesting circuit and LED display. (d) A schematic diagram of the circuit.

associated small-scale mechanical energy and convert it into electricity. Two LEDs connected in antiparallel were sequentially lit up by turning the page back and forth (see video 2†). The corresponding equivalent circuit is illustrated in Fig. 4d. The current and voltage during the page turning were monitored simultaneously, and are depicted in Fig. 4a and b, respectively. It is observed that even the gentle action of turning a book page can generate a current of 4.6 μA at a voltage of 2.4 V. In addition, a Liquid Crystal Display (LCD) could be easily lit up due to its low energy consumption and voltage threshold (see video 3†). This study also indicates that the pNG can serve as an active sensor for detecting mechanical motion/triggering applied to a book page with possible applications in security, document protection and many more.

Conclusion

In summary, using light weight and flexible paper as a substrate, a simple and low-cost paper-based nanogenerator was fabricated, which give a maximum instantaneous power density of ~90.6 μW cm^{-2} by harvesting external mechanical energy, which is enough to light up 70 LEDs. In addition, the pNG has a natural advantage of being able to be attached to other movable objects, such as the pages of a book, and therefore, the harvested mechanical energy from turning a book page could light up LEDs. The successful synthesis of this pNG paves the way in harvesting energy based on electrostatic actuation and this study presents the significant potential applications of a paper-based self-powered system as an energy source or as an active sensor.

Acknowledgements

This work was financially supported by the National Natural Science Foundation of China (51002056, 61204001), a Foundation for the Author of National Excellent Doctoral Dissertation of PR China (201035), and the Program for New Century Excellent Talents in University (NCET-10-0397). The authors thank the facility support of the Center for Nanoscale Characterization & Devices (CNCD), WNLO-HUST.

Notes and references

1 D. Tobjörk and R. Österbacka, *Adv. Mater.*, 2011, **23**, 1935–1961.
2 R. Martins, A. Nathan, R. Barros, L. Pereira, P. Barquinha, N. Correia, R. Costa, A. Ahnood, I. Ferreira and E. Fortunato, *Adv. Mater.*, 2011, **23**, 4491–4496.
3 A. D. Mazzeo, W. B. Kalb, L. Chan, M. G. Killian, J.-F. Bloch, B. A. Mazzeo and G. M. Whitesides, *Adv. Mater.*, 2012, **24**, 2850–2856.
4 A. Russo, B. Y. Ahn, J. J. Adams, E. B. Duoss, J. T. Bernhard and J. A. Lewis, *Adv. Mater.*, 2011, **23**, 3426–3430.
5 F. Eder, H. Klauk, M. Halik, U. Zschieschang, G. Schmid and C. Dehm, *Appl. Phys. Lett.*, 2004, **84**, 2673–2675.
6 L. Hu, H. Wu and Y. Cui, *Appl. Phys. Lett.*, 2010, **96**, 183502–183503.
7 M. Berggren, D. Nilsson and N. D. Robinson, *Nat. Mater.*, 2007, **6**, 3–5.
8 B. Hu, W. Chen and J. Zhou, *Sens. Actuators, B*, 2013, **176**, 522–533.
9 L. Yuan, X. Xiao, T. Ding, J. Zhong, X. Zhang, Y. Shen, B. Hu, Y. Huang, J. Zhou and Z. L. Wang, *Angew. Chem., Int. Ed.*, 2012, **51**, 4934–4938.
10 L. Yuan, B. Yao, B. Hu, K. Huo, W. Chen and J. Zhou, *Energy Environ. Sci.*, 2013, **6**, 470–476.
11 H. Gullapalli, V. S. M. Vemuru, A. Kumar, A. Botello-Mendez, R. Vajtai, M. Terrones, S. Nagarajaiah and P. M. Ajayan, *Small*, 2010, **6**, 1641–1646.
12 K. H. Kim, K. Y. Lee, J.-S. Seo, B. Kumar and S. W. Kim, *Small*, 2011, **7**, 2577–2580.
13 C. Chang, V. H. Tran, J. Wang, Y. K. Fuh and L. Lin, *Nano Lett.*, 2010, **10**, 726–731.
14 X. Chen, S. Xu, N. Yao and Y. Shi, *Nano Lett.*, 2010, **10**, 2133–2137.
15 G. Zhu, R. Yang, S. Wang and Z. L. Wang, *Nano Lett.*, 2010, **10**, 3151–3155.
16 S. Xu, Y. Qin, C. Xu, Y. Wei, R. Yang and Z. L. Wang, *Nat. Nanotechnol.*, 2010, **5**, 366–373.
17 Z. L. Wang and J. Song, *Science*, 2006, **312**, 242–246.
18 J. Kwon, W. Seung, B. K. Sharma, S. W. Kim and J. H. Ahn, *Energy Environ. Sci.*, 2012, **5**, 8970–8975.
19 J. H. Lee, K. Y. Lee, B. Kumar, N. T. Tien, N. E. Lee and S. W. Kim, *Energy Environ. Sci.*, 2013, **6**, 169–175.
20 C. Sun, J. Shi, D. J. Bayerl and X. Wang, *Energy Environ. Sci.*, 2011, **4**, 4508–4512.
21 E. R. Post and K. Waal, *Proc. ESA Annual Meeting on Electrostatics*, 2010, Paper G1.
22 F. Fan, Z. Q. Tian and Z. Lin Wang, *Nano Energy*, 2012, **1**, 328–334.
23 F. Fan, L. Lin, G. Zhu, W. Wu, R. Zhang and Z. L. Wang, *Nano Lett.*, 2012, **12**, 3109–3114.
24 S. Wang, L. Lin and Z. L. Wang, *Nano Lett.*, 2012, **12**, 6339–6346.
25 G. Zhu, C. Pan, W. Guo, C. Y. Chen, Y. Zhou, R. Yu and Z. L. Wang, *Nano Lett.*, 2012, **12**, 4960–4965.
26 J. Zhong, Q. Zhong, F. Fan, Y. Zhang, S. Wang, B. Hu, Z. L. Wang and J. Zhou, *Nano Energy*, 2012, DOI: 10.1016/j.nanoen.2012.11.015.
27 Y. Suzuki, *IEEJ Trans. Electr. Electron. Eng.*, 2011, **6**, 101–111.
28 R. Que, M. Shao, S. Wang, D. D. D. Ma and S. T. Lee, *Nano Lett.*, 2011, **11**, 4870–4873.
29 J. Baland, Y. H. Chao, Y. Suzuki and Y. C. Tai, IEEE the Sixteenth Annual International Conference on Micro Electro Mechanical Systems, Kyoto, 2003, pp. 538–541.
30 R. A. Creswell and M. M. Perlman, *J. Appl. Phys.*, 1970, **41**, 2365–2375.
31 J. A. Giacometti, S. Fedosov and M. M. Costa, *Braz. J. Phys.*, 1999, **29**, 269–279.
32 S. Yoshihiko, S. Yuji and K. Nobuhide, *J. Micromech. Microeng.*, 2008, **18**, 104011–1040116.
33 S. Boisseau, G. Despesse, T. Ricart, E. Defay and A. Sylvestre, *Smart Mater. Struct.*, 2011, **20**, 105013.

34 J. A. Małecki, *Phys. Rev. B: Condens. Matter*, 1999, **59**, 9954–9960.
35 J. A. Cross, *Electrostatics: principles, problems and applications*, Hilger, Bristol, 1987, p xii, p. 500.
36 X. Lu, T. Zhai, X. Zhang, Y. Shen, L. Yuan, B. Hu, L. Gong, J. Chen, Y. Gao, J. Zhou, Y. Tong and Z. L. Wang, *Adv. Mater.*, 2012, **24**, 938–944.
37 L. Y. Yuan, X. Xiao, T. P. Ding, J. W. Zhong, X. H. Zhang, Y. Shen, B. Hu, Y. H. Huang, J. Zhou and Z. L. Wang, *Angew. Chem., Int. Ed.*, 2012, **51**, 4934–4938.
38 L. Y. Yuan, X. H. Lu, X. Xiao, T. Zhai, J. J. Dai, F. C. Zhang, B. Hu, X. Wang, L. Gong, J. Chen, C. G. Hu, Y. X. Tong, J. Zhou and Z. L. Wang, *ACS Nano*, 2012, **6**, 656–661.
39 X. Xiao, T. Ding, L. Yuan, Y. Shen, Q. Zhong, X. Zhang, Y. Cao, B. Hu, T. Zhai, L. Gong, J. Chen, Y. Tong, J. Zhou and Z. L. Wang, *Adv. Energy Mater.*, 2012, **2**, 1328–1332.
40 X. Xiao, T. Li, P. Yang, Y. Gao, H. Jin, W. Ni, W. Zhan, X. Zhang, Y. Cao, J. Zhong, L. Gong, W. C. Yen, W. Mai, J. Chen, K. Huo, Y. L. Chueh, Z. L. Wang and J. Zhou, *ACS Nano*, 2012, **6**, 9200–9206.
41 L. B. Hu and Y. Cui, *Energy Environ. Sci.*, 2012, **5**, 6423–6435.
42 H. Gwon, H. S. Kim, K. U. Lee, D. H. Seo, Y. C. Park, Y. S. Lee, B. T. Ahn and K. Kang, *Energy Environ. Sci.*, 2011, **4**, 1277–1283.
43 L. Y. Yuan, B. Yao, B. Hu, K. F. Huo, W. Chen and J. Zhou, *Energy Environ. Sci.*, 2013, **6**, 470–476.
44 L. Qie, W. M. Chen, Z. H. Wang, Q. G. Shao, X. Li, L. X. Yuan, X. L. Hu, W. X. Zhang and Y. H. Huang, *Adv. Mater.*, 2012, **24**, 2047–2050.
45 L. Hu, J. W. Choi, Y. Yang, S. Jeong, F. La Mantia, L. F. Cui and Y. Cui, *Proc. Natl. Acad. Sci. U. S. A.*, 2009, **106**, 21490–21494.
46 L. B. Hu, G. Y. Zheng, J. Yao, N. Liu, B. Weil, M. Eskilsson, E. Karabulut, Z. C. Ruan, S. H. Fan, J. T. Bloking, M. D. McGehee, L. Wagberg and Y. Cui, *Energy Environ. Sci.*, 2013, **6**, 513–518.

